RADIATION RESEARCH **84,** 189–218 (1980)

Measurement of *W* Values of Low-Energy Electrons in Several Gases

D. COMBECHER

Gesellschaft fuer Strahlen- und Umweltforschung, Institut fuer Strahlenschutz,
Neuherberg 8042, West Germany

COMBECHER, D. Measurement of *W* Values of Low-Energy Electrons in Several Gases. *Radiat. Res.* **84,** 189–218 (1980).

The *W* value, the mean energy required to form an ion pair, was measured for monoenergetic electrons in the energy range from 5 to about 500 eV in air, N_2, O_2, CO_2, tissue-equivalent gases (Rossi–Failla and Srdoc mixtures), methane, ethane, propane, *n*-butane, i-butane, pentane, hexane, nonane, ethylene, acetylene, ethanol, acetone, H_2O, D_2O, H_2, D_2, C_6H_6, C_6D_6, argon, krypton, and xenon. The *W* values of all gases increase continuously with decreasing electron energy; they approach infinity asymptotically at the ionization thresholds and the well-known energy-independent high-energy *W* values at high electron energies. A comparison between the results and newer experimental and theoretical works of other authors sometimes shows very good agreement. The experimental error is estimated to be less than 2%.

INTRODUCTION

The *W* value of an energetic charged particle is the mean energy expended by the particle to form an ion pair. It is the ratio of the starting energy of the particle to the mean number of ions produced when it is completely stopped in the absorbing material.

Knowledge of low-energy electron *W* values is important for three reasons. First, they are a useful tool to verify theoretical radiation-transport calculations for low-energy electrons which play an important role in energy deposition processes but are difficult to calculate, as the Bethe approximation is not valid for low energies and complete and accurate sets of excitation and differential ionization cross sections are not available. Second, they are needed for the calculation of the absorbed energy from the measured number of ions produced in microdosimetric experiments. Third, if the stopping power and the differential ionization cross sections $\sigma(T,E)$ are known for high-energy ions, they allow the calculation of high-energy ion *W* values which are needed for dosimetric measurements.

Whereas the *W* values of high-energy electrons are well known for the most convenient gases, for electrons below 1 keV little work, quoted later in comparison with our own results, has been done until now, and much of it is contradictory. The reason for this is that some experimental difficulties appear in addition to those in high-energy *W*-value measurements. The special problems for low-energy measurements are

0033-7587/80/110189-30$02.00/0

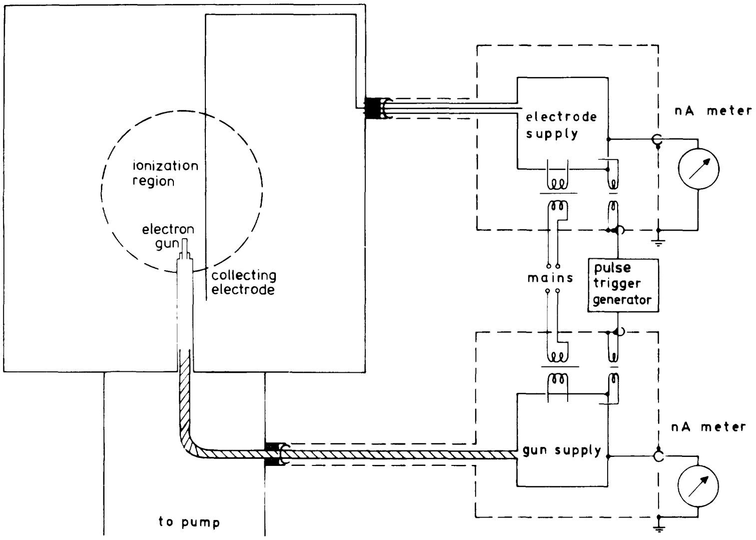

FIG. 1. Experimental apparatus.

(1) the production of low-energy electrons in a gas and the precise measurement of their number;

(2) the avoidance of energy falsification by an electric field needed for ion collection, and by contact potentials and surface charges.

To overcome these difficulties an apparatus was constructed differing in some details from those used in earlier investigations.

EXPERIMENTAL

For the measurement of *W* values two quantities must be determined: the energy supplied to the gas by electrons and the number of ions produced in the gas. The electrons are produced by a gun, and the number of ions is determined by measurement of the current in an ion collecting electrode. The experimental apparatus is shown in Fig. 1. It consists of a stainless-steel ion chamber 45 cm long and 45 cm in diameter with a thin ion collector wire 0.2 mm in diameter set off-axis by 3 cm. At the bottom of the chamber the electron gun is mounted on a 15-cm-long, 2-cm-diameter brass tube. The gun is constructed very compactly; it is not pumped (Fig. 2). It consists of a cathode, a Wehnelt cylinder, an anode, and a shielding electrode. The cathode is a 0.2-mm iridium wire squeezed into 1-mm copper wires. The insulators are ceramic tubes glued to the electrodes with ceramic powder. The distance between the cathode and the outermost electrode is only 3 mm. This gun yields 10^{-5} A down to 5 eV electron energy. All electrodes of the gun as well as the vacuum chamber are coated with a thin carbon layer for protection from undesired charges.

The compact design of the gun reduces the influence of effects inside the gun and prevents electrons from touching any electrode. Figure 3 shows some calculated electron paths for the worst cases, namely, for electrons starting eccentric with

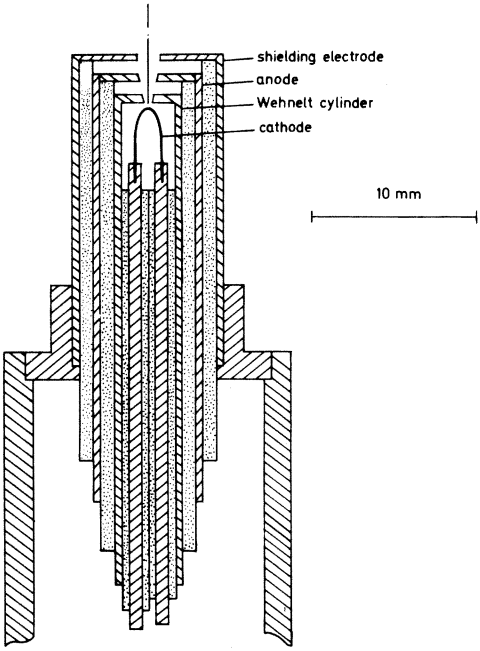

FIG. 2. Electron gun.

0.1 eV accelerated to 250 eV and for those starting with 1.5 eV accelerated to 15 eV, with the Wehnelt cylinder held on cathode potential. In the measurements a small negative potential with respect to the cathode is applied to the Wehnelt cylinder to focus the emitted electrons somewhat more.

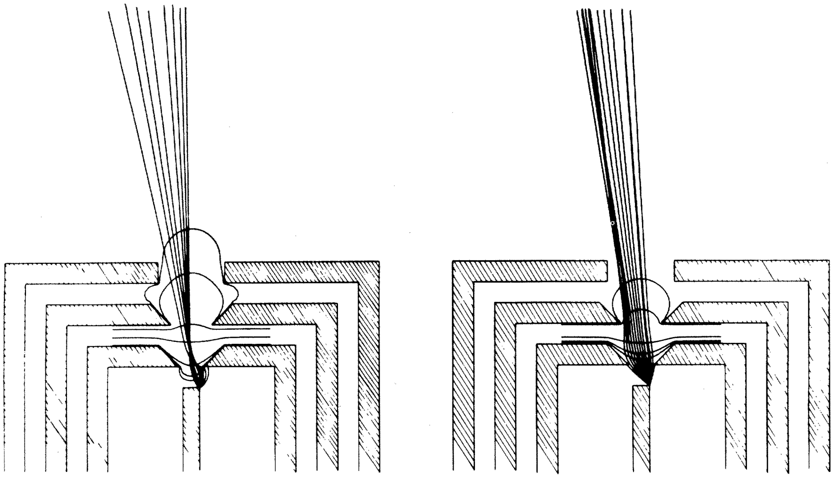

FIG. 3. Left: Pathways of electrons accelerated to 250 eV. The equipotential lines are drawn for −249, −248, −240, −150, −50, −1, and −0.1 V. Right: Pathways of electrons accelerated to 15 eV. The equipotential lines are drawn for −14, −13, −10, −1, and −0.1 V.

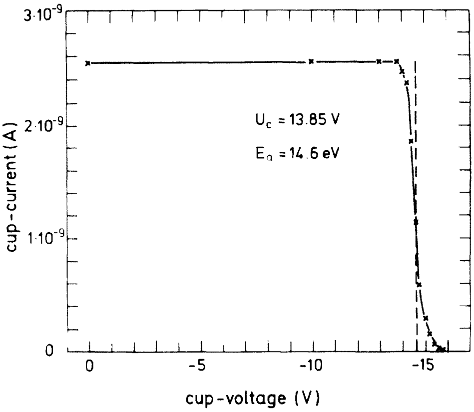

FIG. 4. Dependence of the Faraday cup current on the retarding cup voltage at a cathode voltage of 13.85 eV.

The anode is connected to ground potential via a nA-meter. The gun and the gun supply are highly insulated against ground potential so that the current leaving the anode is identical to the nA-meter current. The anode is surrounded by a grounded shielding electrode; thus it cannot be reached by charged particles produced in the measuring chamber. The mains transformer in the gun supply is specially made with a resistance of 10^{14} ohms between the primary and secondary coils. A leakage current of less than 10^{-13} A was achieved by using highly insulating materials and the consistent application of the usual guard-ring techniques.

The gun was tested under vacuum with a retarding-field Faraday cup coated with a thin carbon layer. Figure 4 shows the cup current versus the negative cup voltage at 13.85 V cathode voltage. The tests showed that the average energy of the emitted electrons is 0.75 eV higher than the negative voltage applied to the cathode because of the thermal energy of the electrons leaving the cathode filament and the contact potential between the iridium cathode and the carbon layer of the cup. The contact potential between the cathode and the Faraday cup is the same as that between the cathode and the experimental chamber, since the chamber and the cup are coated with the same carbon material. It should be low since the work functions of iridium and carbon are close together (near 4.5 eV) (*1*). When the cup potential was more positive than the filament potential, no difference was found between the cup current and the nA-meter current; when it was more negative than the filament potential by at least 2 V the cup current was zero. This is supporting evidence that

(1) no electrons lose energy by scattering at the diaphragms;

(2) no undesired charges are produced on the carbon coated surfaces;

(3) the current measuring method is correct.

The measurement of the ion current is carried out by the same method. A negative voltage of 60 V is applied to the ion collector wire. The problem of avoiding the falsification of the electron energy by the electric field produced by the collector wire is solved by synchronously pulsing the collector voltage and the electron current (Fig. 5). Every 100 μsec the collector voltage is shorted to ground potential.

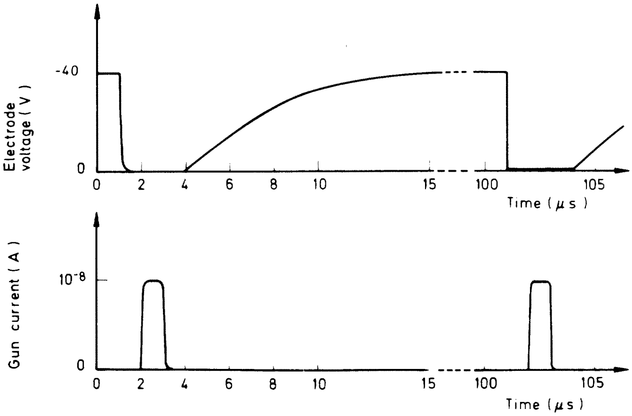

FIG. 5. Pulse diagram of the electron gun current and the ion collector voltage.

At the same time a 1-μsec electron pulse is emitted into the fieldless chamber by increasing the Wehnelt potential from -15 V to an adjustable value (ca. -1 V) with respect to the cathode. The electrons are stopped in the gas within 1 μsec after emission to an energy below the ionization thresholds since the velocity of electrons with higher energy is greater than 150 cm/μsec. Electrons with lower energy do not contribute to the measured signal. The collector voltage rises slowly, 1.5 μsec after the electron pulse, so that the electrons in the proximity of the collector are drawn out of the region of high field strength.

The measurement of the electron gun current is correct only if the gun is under vacuum, but for measurement of the *W* values the measuring chamber must be filled with gas with a pressure of 10–100 μbar. Since the gun is not pumped, scattering of electrons within the electrode system and ion collection by the cathode resulting from the formation of ions within the electric field of the gun will falsify the energy of the electrons leaving the gun and the measurement of the electron current. This is shown in Fig. 6. In this example, for 26.7-eV electrons entering H_2O, the ratio of the ion collector current to the measured gun current is plotted against the gas pressure in the chamber. At low pressures, where the range of the electrons is larger than the chamber length, the ratio rises with pressure. After passing through a maximum the curve decreases slowly, since events inside the gun become more significant with rising pressure. It may be shown that this decrease should be linear for low pressures and low electron energies. The number of electrons scattered and that of ions collected by the gun assembly should be proportional to pressure when only a small part of the electron energy is lost within the electron gun. This condition is fulfilled because the range of the electrons under measuring conditions is 100–300 mm, whereas the pathway inside the gun is only 3 mm. The measured ion current i is lower than the current i_0 of the produced ions due to the ion collection by the cathode at a rate of $k_1 \cdot p$, and the measured gun current e is higher than the current e_0 of electrons leaving the gun due to the ion collection and the scattering of primary electrons toward the gun electrodes at a rate of $k_2 \cdot p$, where p is the pressure,

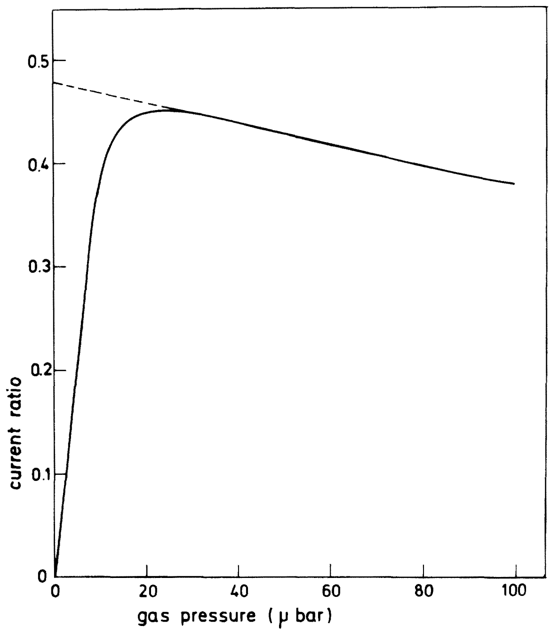

FIG. 6. Pressure dependence of the ratio of the ion collector current to the gun current.

$$i = i_0 \cdot (1 - k_1 \cdot p),$$

$$e = e_0 \cdot (1 + k_2 \cdot p) + i_0 \cdot k_1 \cdot p,$$

with

$$i_0 = e_0 \cdot E/W.$$

The measured ratio is

$$\frac{i}{e} = \frac{E}{W} \cdot \frac{1 - k_1 \cdot p}{1 + k_2 \cdot p + E/W \cdot k_1 \cdot p},$$

with $k_1 \cdot p, k_2 \cdot p \ll 1$, it is approximately

$$\frac{i}{e} \approx \frac{E}{W} \cdot (1 - k_1 \cdot p - k_2 \cdot p - E/W \cdot k_1 \cdot p + (E/W \cdot k_1 + k_2)^2 \cdot p^2).$$

The quadratic term in this equation may be neglected for low energies and pressures. In the experiments the decrease of the ratio has been found to be linear with pressure over a wide range, so that it is possible to extrapolate it to zero pressure. At zero pressure all effects inside the gun which falsify the measurements vanish. Therefore the extrapolated ratio is taken to calculate the W value.

To avoid impurities in the investigated gases the apparatus is regularly baked out at ca. 130°C. The turbomolecular pump evacuating the chamber is protected against forepump oil by an aluminium oxide filter. The gas supply valves and pipes are flushed and evacuated before filling, and liquids are degassed for some time before the start of the measurements.

The maximum amounts of impurities indicated by the manufacturers of the investigated gases (Linde AG) and liquids (Merck AG) are: Ar: 0.0005%; N_2, H_2,

H_2O: 0.001%; Xe: 0.003%; O_2, CO_2: 0.005%; Kr: 0.01%; CH_4: 0.05%; ethylene, ethanol: 0.2%; D_2, D_2O, benzene: 0.3%; acetylene: 0.4%; acetone, propane, butane, C_6D_6: 0.5%; ethane, pentane, hexane: 1%; nonane: 2%. An additional impurity is caused by the leakage and outgassing of the experimental chamber. The measured leakage and outgassing rate is 5×10^{-7} mbar/sec, and the sample gas flow rate into the chamber is 5×10^{-3} mbar/sec, so the additional impurity by leakage and outgassing is 0.01%.

The control of the experiment and the data acquisition are achieved by a laboratory computer. Before every *W*-value measurement the measuring chamber is evacuated to 10^{-5} mbar by a turbomolecular pump. Then the pump valve is closed and a steady gas flow into the chamber is maintained by opening a controllable valve, so that the pressure in the chamber rises linearly with time. The nA-meters are connected to voltage-frequency converters and their outputs are fed to scalers. The contents of the scalers are read every 0.4 sec by the computer. At the end of the measurement the ratio of the currents is plotted against the gas pressure while the ionization chamber is evacuated again. The automatic setup allows the easy measurement of a great number of *W* values with reproducible experimental conditions.

RESULTS

The experimental results are shown in Table I and Figs. 7–15. They show a continuous decrease of the *W* values with increasing electron energy. At low energy they approach infinity asymptotically near the ionization thresholds of the investigated gases, and at high energies they approach the well-known constant high-energy electron *W* value. The results reported in an earlier work (*2*) are included. The ionization thresholds and the high-energy *W* values are marked in the figures. These values are summarized in Table II. The ionization thresholds are taken from the extensive compilations by Kiser (*3*) and Rosenstock *et al.* (*4*). Preferably those measured with the photoionization method are selected. The *W* values are averaged over the values reported by different authors.

The data points in the figures generally are connected with straight lines, and only a few of them are indicated by symbols to improve the clearness of the figures.

Figure 7 shows the results for dry air and its components. The *W* values of air are very similar to those of N_2. The curves for O_2 and CO_2 show different shapes; they cross twice.

Figure 8 shows the results for the tissue-equivalent gas mixture proposed by Rossi and Failla in comparison with its components. It consists of 64.4% methane, 32.4% CO_2, and 3.2% N_2. The results are close to those for methane.

Figure 9 shows the results for the tissue-equivalent gas mixture proposed by Srdoc in comparison with its components. It consists of 55% propane, 39.6% CO_2, and 5.5% N_2. The results are determined mainly by the propane. The data for this gas mixture presented in (*2*) were wrong; probably the gas in the former measurements had been decomposed.

Figure 10 shows the results for several alkanes. There is a continuous change between ethane and nonane; the results are very close to each other with the excep-

TABLE I

Measured W Values for Several Gases

Energy	*W Value*	*Energy*	*W Value*	*Energy*	*W Value*	*Energy*	*W Value*
Air		N_2		O_2		CO_2	
14.7	1901.75	15.8	1030.38	12.2	1712.67	13.6	1655.66
15.7	640.43	16.1	639.05	12.7	727.98	14.1	526.24
16.7	336.69	16.6	439.18	13.7	361.63	14.6	321.22
17.7	232.71	17.1	338.87	14.7	274.40	15.1	210.49
18.7	176.30	17.7	265.92	15.7	220.32	15.6	175.52
19.7	147.32	18.7	193.35	16.7	181.72	16.7	135.36
20.7	125.56	19.7	155.61	17.7	151.46	17.6	116.64
22.7	106.81	20.7	132.19	18.7	134.48	18.7	104.66
24.7	93.31	21.7	118.49	19.7	121.68	19.7	94.79
26.7	82.12	22.7	107.71	20.7	105.24	20.7	89.49
28.7	75.89	24.7	95.01	22.7	91.15	21.6	84.00
30.7	70.44	26.7	84.30	24.7	79.99	22.7	80.57
32.7	66.18	28.8	77.77	26.7	72.05	23.7	76.69
34.7	63.72	30.7	72.21	28.7	66.19	24.7	74.02
36.7	60.14	32.7	68.34	30.7	61.48	26.7	69.14
38.7	59.15	34.7	64.24	32.7	58.04	28.7	62.77
40.7	57.82	36.7	60.82	34.7	55.52	30.7	58.98
45.7	54.44	38.7	59.30	36.7	53.14	32.7	57.19
50.7	51.32	40.7	57.46	38.7	51.58	34.7	54.20
60.7	47.96	45.7	54.52	40.7	49.82	36.7	52.34
80.7	44.32	50.7	51.77	45.7	46.88	38.7	2.34
100.7	42.45	60.7	48.91	50.7	44.76	40.7	50.86
120.7	41.29	70.7	46.49	60.7	41.72	45.7	48.38
150.7	39.62	80.7	45.08	70.7	39.66	50.7	47.36
200.7	38.73	100.7	43.26	80.7	38.42	60.7	44.16
250.7	38.21	125.7	41.79	90.7	37.14	70.7	42.47
300.7	37.88	150.7	41.03	100.7	36.59	80.7	41.51
350.7	37.65	200.7	39.91	150.7	34.71	90.7	40.72
400.7	37.33	250.7	39.23	175.7	33.83	100.7	40.33
450.7	37.47	300.7	38.72	200.7	33.25	125.7	39.70
500.4	36.81	350.7	38.83	300.7	32.55	150.7	38.63
700.0	36.09	400.7	38.39			175.7	38.58
1000.0	35.54	450.7	37.88			200.7	38.41
		500.0	37.62			250.7	38.17
		700.0	36.82			300.7	38.26
		1000.0	36.68			350.7	38.15
						400.7	37.66
TE Gas							
Rossi Mixture		Srdoc mixture		Methane		Ethane	
13.7	1679.51	12.7	707.00	13.9	901.79	12.7	1019.84
14.0	765.72	13.7	243.00	14.2	546.62	13.2	332.96
14.7	305.38	14.7	114.39	14.6	309.86	13.6	233.20
15.7	158.44	15.7	73.27	14.9	234.58	14.2	132.07
16.7	106.14	16.7	60.35	15.1	186.71	14.7	95.02
17.7	85.60	17.7	53.40	15.9	118.35	15.7	67.60

TABLE I—*Continued*

Energy	*W Value*	*Energy*	*W Value*	*Energy*	*W Value*	*Energy*	*W Value*
TE Gas							
Rossi mixture		Srdoc mixture		Methane		Ethane	
18.7	73.45	18.7	49.99	16.7	90.68	16.7	54.90
19.7	67.65	19.7	47.55	17.7	72.67	17.7	48.51
20.7	63.00	20.7	46.08	18.7	64.33	18.7	44.81
22.7	58.60	22.8	44.06	19.6	57.83	19.6	42.58
24.7	55.72	24.7	42.65	20.7	54.84	20.6	41.02
26.7	52.97	26.7	41.11	22.7	51.02	22.7	39.71
28.7	50.38	28.7	39.58	24.7	48.31	24.7	38.93
30.7	47.81	30.7	38.08	26.7	46.92	26.7	37.68
32.7	45.83	32.7	36.92	28.7	45.33	28.7	36.52
34.7	44.21	34.7	36.38	30.7	43.53	30.7	35.10
36.7	43.49	36.7	35.70	32.7	41.60	32.7	34.60
38.7	42.75	38.7	35.01	34.7	40.72	34.7	33.74
40.7	41.84	40.7	34.84	38.7	39.28	36.7	33.16
45.7	40.50	45.7	33.60	40.7	38.66	38.7	32.82
50.7	38.69	50.7	33.01	45.7	37.70	40.7	32.46
60.7	37.50	60.7	31.90	50.7	37.11	45.7	31.65
70.7	36.35	70.7	31.25	70.7	34.21	50.7	31.19
80.7	35.69	80.7	30.53	100.7	32.26	60.7	30.26
100.0	34.40	90.7	30.25	150.7	30.54	70.7	29.74
130.0	32.52	100.7	29.88	200.7	30.55	80.7	29.32
160.0	32.26	130.0	29.56	250.7	29.70	90.7	29.07
200.0	31.82	150.7	29.30			100.7	28.71
250.0	31.70	175.7	29.28			125.7	27.88
300.0	32.21	200.0	28.52			150.7	27.53
350.0	31.32	250.0	28.66			175.7	27.37
400.0	31.78	300.0	28.78			200.7	27.07
500.0	31.48	350.0	28.61			250.7	26.90
600.0	31.70	400.0	28.43				
700.0	31.23	500.0	28.63				
800.0	31.23	600.0	28.45				
1000.0	30.87	700.0	28.44				
1200.0	30.75	800.0	28.33				
		1000.0	28.54				
Propane		*n*-Butane		i-Butane		*n*-Pentane	
11.7	1938.76	11.9	1398.60	12.2	557.08	12.2	541.83
12.0	813.10	12.2	666.29	12.7	261.88	12.7	268.71
12.2	558.47	12.7	289.36	13.2	174.33	13.2	153.23
12.4	379.69	13.2	162.00	13.7	117.91	13.6	108.92
12.7	272.75	13.7	113.15	14.1	93.35	14.1	82.34
12.9	197.71	14.1	88.53	14.6	75.49	14.7	66.82
13.4	140.93	14.7	69.81	15.6	58.35	15.7	50.77
13.9	98.91	15.6	55.31	16.6	49.52	16.6	44.94
14.7	72.14	16.7	46.64	17.6	43.76	17.7	40.80
15.7	56.46	17.7	42.13	18.7	41.69	18.7	38.61
16.7	48.55	18.7	40.13	19.7	40.18	19.6	37.48
17.7	43.71	19.7	38.75	20.7	39.41	20.6	36.99

TABLE I—*Continued*

Energy	*W Value*	*Energy*	*W Value*	*Energy*	*W Value*	*Energy*	*W Value*
Propane		*n*-Butane		i-Butane		*n*-Pentane	
18.7	41.71	20.7	38.49	22.7	38.30	22.7	36.03
19.7	40.29	22.7	37.15	24.7	37.19	24.7	35.45
20.7	39.33	24.7	36.43	25.7	36.58	26.7	34.34
22.7	38.84	25.7	35.91	26.7	36.20	28.7	32.90
24.7	37.70	26.7	35.01	28.7	34.84	30.7	32.33
26.7	36.42	28.7	34.03	30.7	33.50	32.7	31.84
28.7	35.08	30.7	33.30	32.7	33.33	34.7	31.05
30.7	34.13	32.7	32.63	34.7	32.80	36.7	30.91
32.7	33.66	34.7	32.06	36.7	32.28	38.7	30.41
34.7	32.96	36.7	31.39	38.7	31.80	40.7	29.95
36.7	32.33	38.7	31.26	40.7	31.21	45.7	29.60
38.7	32.15	40.7	30.58	45.7	31.00	50.7	28.84
40.7	32.06	45.7	30.32	50.7	30.53	60.7	28.42
45.7	31.23	50.7	29.78	60.7	29.40	70.7	27.92
50.7	30.56	60.7	29.02	70.7	29.10	80.7	27.57
70.7	29.38	70.7	28.78	80.7	28.85	90.7	27.47
100.7	28.48	80.7	28.20	90.7	28.13	100.7	27.17
130.7	27.99	90.7	28.46	100.7	28.45	125.7	27.05
160.7	27.65	100.7	27.89	125.7	27.34	150.7	26.42
200.7	27.33	125.7	27.30	150.7	27.41	175.7	26.52
250.7	26.95	150.7	27.23	175.7	27.22	200.7	26.25
		175.7	26.98	200.7	26.78	250.7	25.92
		200.7	27.34			300.7	25.81
		250.7	26.37			350.7	25.83
		300.7	26.35				
		350.7	26.47				
n-Hexane		*n*-Nonane		Ethylene		Acetylene	
12.2	333.22	11.6	742.95	12.2	346.55	12.1	929.46
12.6	182.75	12.2	304.13	12.7	249.68	12.6	288.70
13.1	125.88	12.7	163.35	13.2	183.63	13.2	171.58
13.7	90.45	13.7	83.82	13.7	157.35	13.7	122.87
14.2	72.34	14.7	56.32	14.2	129.57	14.2	103.12
14.7	59.62	15.7	46.42	14.7	110.08	14.7	86.61
15.7	48.52	16.7	40.84	15.7	90.31	15.1	75.10
16.7	42.97	17.6	38.08	16.7	75.29	15.6	69.42
17.7	39.43	18.7	36.70	17.7	68.68	16.2	60.71
18.7	37.59	19.7	35.70	18.7	62.75	16.7	58.91
19.7	36.02	20.7	35.62	19.7	59.14	17.6	55.22
20.7	36.22	21.7	34.93	20.7	54.89	18.7	53.75
22.7	35.40	22.7	34.99	22.7	49.69	19.7	52.08
24.7	34.36	23.7	34.11	24.7	46.16	20.7	50.58
26.7	33.05	24.7	33.67	26.7	44.94	22.7	46.31
28.7	32.34	25.7	33.26	28.7	41.90	24.7	43.33
30.7	31.26	26.7	32.62	30.7	40.86	26.7	41.01
32.7	30.82	28.7	31.90	32.7	39.61	28.7	38.94
34.7	30.70	30.7	31.07	34.7	38.81	30.7	37.47
36.7	30.19	32.7	30.31	36.7	37.89	32.7	36.60
38.7	29.71	34.7	30.48	38.7	36.80	34.7	35.86

TABLE I—*Continued*

Energy	*W Value*	*Energy*	*W Value*	*Energy*	*W Value*	*Energy*	*W Value*
n-Hexane		*n*-Nonane		Ethylene		Acetylene	
40.7	29.82	36.7	29.35	40.7	36.73	36.7	35.68
45.7	29.06	38.7	29.47	45.7	35.79	38.7	34.96
50.7	28.64	40.7	29.27	50.7	34.08	40.7	34.48
60.7	28.24	45.7	28.83	60.7	32.68	45.7	33.00
70.7	27.66	50.7	28.24	70.6	32.23	50.7	32.42
80.7	27.23	60.7	27.89	80.8	31.60	60.7	32.60
90.7	27.33	70.7	27.00	90.7	31.02	70.7	31.15
100.7	27.03	100.7	26.67	100.7	30.59	80.7	30.94
125.7	26.45	150.7	26.28	125.7	29.71	90.7	30.46
150.7	26.12	175.7	26.01	150.7	29.37		
175.7	25.69	200.7	25.83	175.7	29.38		
		250.7	25.59	200.7	28.75		
		300.7	25.40				
		350.7	25.19				
		400.7	25.18				
		450.7	25.22				
Ethanol		Acetone		H_2		D_2	
12.1	810.85	11.7	521.41	15.7	456.94	15.7	428.97
12.7	362.92	12.7	250.59	16.1	286.36	16.2	256.72
13.7	161.98	13.7	162.73	16.7	210.19	16.6	197.25
14.7	98.75	14.7	114.40	17.1	164.65	17.2	153.28
15.7	72.71	15.7	88.50	17.7	137.51	17.7	130.15
16.7	60.44	16.7	74.71	18.1	120.67	18.1	115.97
17.7	53.29	17.7	64.97	18.6	110.63	18.7	103.55
18.7	48.86	18.6	58.91	19.7	93.30	19.2	96.56
19.7	46.70	19.7	54.69	20.7	85.61	19.6	91.63
20.6	45.18	20.6	51.55	21.7	80.40	20.7	83.63
21.7	44.04	21.6	49.30	22.7	77.02	21.7	78.96
22.7	42.74	22.7	48.02	24.7	72.70	22.7	75.78
23.7	41.93	23.7	47.35	26.7	70.57	24.7	73.18
24.7	41.38	24.7	44.63	28.7	67.46	26.7	70.50
25.7	40.74	25.7	43.61	29.0	66.63	28.7	67.78
26.6	40.06	26.7	42.73	29.3	65.74	29.0	66.20
28.7	38.13	28.7	41.61	29.6	65.17	29.3	66.09
30.7	36.95	30.7	39.39	29.9	64.51	29.6	64.95
32.7	36.23	32.7	38.63	30.2	63.87	29.9	64.69
34.7	35.35	34.7	37.93	30.5	62.91	30.2	63.73
36.7	34.82	36.7	37.19	30.9	62.01	30.5	63.00
38.7	34.38	38.7	36.46	32.7	59.36	30.7	62.60
40.7	34.15	50.7	34.33	34.7	57.36	32.7	60.21
45.7	33.29	60.7	32.84	36.7	55.48	34.7	57.13
50.7	32.33	70.7	31.88	38.7	54.82	36.7	55.54
60.7	31.89	80.7	31.65	40.7	53.73	38.7	54.15
70.7	31.15	90.7	31.22	45.7	50.87	40.7	53.84
80.7	30.21	100.7	31.02	50.7	49.02	45.7	51.27
90.7	30.18	125.7	30.36	70.7	44.73	50.7	49.34
100.7	29.82	150.7	29.98	100.7	42.20	70.7	45.18
125.7	29.24	175.7	29.71	150.7	40.50	100.7	42.32

TABLE I—*Continued*

Energy	*W Value*	*Energy*	*W Value*	*Energy*	*W Value*	*Energy*	*W Value*
Ethanol		Acetone		H_2		D_2	
150.7	28.96	200.7	29.64	200.7	41.16	150.7	40.87
175.7	28.89	250.7	29.28	250.7	39.75	200.7	39.91
200.7	28.60	300.7	28.78	300.7	39.09	250.7	39.31
250.7	28.39	350.7	28.88	350.7	38.94	300.7	39.35
300.7	28.31	400.7	28.43	400.7	38.98	350.7	38.99
350.7	27.96	500.7	28.30	500.7	38.64	400.7	39.02
400.7	27.75					450.7	39.06
450.7	27.56					500.7	38.92
500.7	27.60						
H_2O		D_2O		C_6H_6		C_6D_6	
12.7	662.95	12.6	1039.39	10.6	807.10	10.2	940.74
13.2	483.68	13.2	500.83	11.2	352.46	10.7	433.68
13.7	290.66	13.7	263.32	11.6	248.29	11.1	297.37
14.1	207.09	14.2	194.91	12.2	186.21	11.7	201.42
14.7	166.96	14.7	154.18	12.7	151.99	12.1	164.40
15.6	118.65	15.2	127.62	13.4	115.92	12.6	13.81
16.6	99.17	15.7	109.34	14.0	99.88	13.1	110.79
17.7	86.15	16.7	91.00	14.7	87.73	13.7	97.75
18.7	79.59	17.6	82.48	15.7	73.48	14.1	90.12
19.7	72.87	18.7	74.61	16.7	65.52	14.7	80.50
20.7	68.46	19.7	69.19	17.7	59.87	15.7	68.79
22.7	62.74	20.7	65.76	18.7	54.76	16.7	62.74
24.7	58.32	21.7	62.72	19.7	51.75	17.7	56.61
26.7	55.47	22.6	60.41	20.7	48.17	18.7	51.73
28.7	52.13	23.7	58.85	22.7	43.65	19.7	47.91
30.7	50.13	24.7	56.11	24.7	41.66	20.7	45.70
32.7	48.37	26.7	52.98	26.7	38.83	22.7	41.81
34.7	47.00	28.7	50.37	28.7	37.23	24.7	39.56
36.7	45.39	30.7	48.51	30.7	36.47	26.7	37.80
38.7	44.85	32.7	46.66	32.7	35.62	28.7	36.73
40.7	44.17	34.7	45.32	34.7	34.94	30.7	35.61
45.7	42.06	36.7	44.63	36.7	33.92	32.7	34.95
50.7	40.63	38.7	43.70	38.7	33.66	34.7	34.07
60.7	39.04	40.7	42.52	40.7	33.45	36.7	33.60
70.7	37.46	45.7	41.03	45.7	32.48	38.7	33.24
80.7	36.67	50.7	39.89	50.7	32.10	40.7	32.94
90.7	35.99	60.7	38.11	60.7	30.99	45.7	31.65
100.7	35.15	70.7	37.12	70.7	30.33	50.7	31.08
125.7	34.13	80.7	35.99	80.7	29.92	60.7	30.46
150.7	33.89	90.7	35.48	90.7	29.47	70.7	29.86
175.7	33.28	100.7	34.91	100.7	29.59	80.7	29.45
200.7	32.70	125.7	33.83	125.7	28.92	90.7	29.41
250.7	32.40	150.7	33.13	150.7	29.06	100.7	29.12
300.7	32.03	175.7	32.73	175.7	28.09	125.7	28.62
350.7	31.75	200.7	32.30	200.7	28.64	150.7	28.57
400.7	31.29	250.7	31.78			175.7	28.57
450.7	31.14	300.7	31.20			200.7	28.26
500.0	30.89	350.7	31.10				

TABLE I—*Continued*

Energy	*W Value*	*Energy*	*W Value*	*Energy*	*W Value*	*Energy*	*W Value*
H_2O		D_2O		C_6H_6		C_6D_6	
500.7	30.93	400.7	30.80				
600.0	30.53	450.7	30.65				
700.0	30.78	500.7	30.43				
800.0	30.61						
900.0	30.38						
Argon		Krypton		Xenon			
14.6	3086.94	13.0	2988.19	11.2	900.00		
15.2	634.35	13.3	845.06	11.7	186.00		
15.6	246.80	13.7	262.64	12.2	107.00		
16.2	149.76	14.7	102.45	12.7	82.40		
16.7	112.66	15.7	66.39	13.8	56.30		
17.6	76.20	16.7	54.54	15.7	43.40		
18.6	61.11	17.7	48.82	17.8	39.90		
19.6	54.07	18.7	45.94	20.7	37.70		
20.7	49.86	19.7	43.70	25.7	32.70		
21.6	48.05	20.7	42.69	30.7	30.80		
22.6	46.38	22.7	42.12	40.8	28.50		
23.7	45.46	24.7	41.29	50.8	27.44		
24.7	45.46	26.7	39.13	70.7	26.20		
25.7	44.78	28.7	37.17	100.8	25.38		
26.7	45.22	30.7	35.30	150.0	24.62		
27.7	44.71	32.7	34.47	200.0	24.25		
28.7	44.38	34.7	33.77	250.0	24.56		
29.7	43.61	36.7	33.44	500.0	24.39		
30.7	42.57	38.7	32.87	1000.0	23.78		
32.7	40.80	40.7	32.60				
34.7	38.73	45.7	31.60				
36.7	38.11	50.7	30.94				
38.7	37.49	60.7	29.99				
40.7	37.26	70.7	29.36				
45.7	36.43	80.7	28.78				
50.7	35.57	100.7	28.17				
60.7	34.38	125.7	27.59				
70.7	33.54	150.7	27.41				
80.7	32.82	175.7	27.33				
90.7	32.33	200.7	27.16				
100.7	32.14	250.7	27.14				
125.7	31.85	300.7	26.90				
150.7	30.99						
175.7	30.62						
200.7	30.43						
250.7	29.83						
300.7	29.70						
350.7	29.14						
400.7	29.06						
450.7	29.18						
500.7	29.03						

TABLE II

Ionization Threshold and High-Energy Electron *W* Value

Gas	*Ionization threshold (eV)*	*High energy W value (eV)*
Air	See O_2	33.9 (*54, 55*)
N_2	15.572 (*41*)	34.8 (*54–57*)
O_2	12.075 (*42*)	30.8 (*54–57*)
CO_2	13.767 (*43*)	33.0 (*54–60*)
TE gas (Rossi mixture)	See methane	29.2[a]
TE gas (Srdoc mixture)	See propane	26.1[a]
Methane	12.55 (*44*)	27.3 (*54, 56–61*)
Ethane	11.521 (*45*)	25.0 (*54, 57–59, 61*)
Propane	10.95 (*46*)	24.0 (*57–59, 61*)
n-Butane	10.63 (*47*)	23.4 (*57–59, 61*)
i-Butane	10.57 (*47*)	
n-Pentane	10.35 (*47*)	23.2 (*57, 58, 61*)
n-Hexane	10.18 (*47*)	23.0 (*57, 61*)
n-Nonane	10.21 (*48*)	
Ethylene	10.515 (*42*)	25.8 (*54, 56, 59, 61*)
Acetylene	11.41 (*49*)	25.8 (*54, 58, 61*)
Ethanol	10.48 (*47*)	24.8 (*57, 61*)
Acetone	9.690 (*42*)	
H_2	15.42 (*50*)	36.4 (*54, 56, 58*)
D_2	15.47 (*51*)	
H_2O	12.614 (*44*)	29.6 (*57, 59, 62*)
D_2O	12.637 (*44*)	
C_6H_6	9.247 (*52*)	22.1 (*58, 59*)
C_6D_6	9.251 (*52*)	
Argon	15.759 (*53*) 14.71[b] (*12*)	26.4 (*54, 55, 57*)
Krypton	13.999 (*45*) 13.004[b] (*12*)	24.3 (*54–56*)
Xenon	12.129 (*45*) 11.162[b] (*12*)	22.0 (*54–56*)

---

[a] Calculated from the *W* values and the concentrations of the components using the formula and the constants given by Strickler (*37*)—modified for ternary mixtures—for α particles. The assumption that the constants for electrons are the same should be valid within small error margins since the stopping power ratios in the various components of the TE gases are similar for high-energy α particles and electrons. The *W* value calculated for the Rossi–Failla mixture is identical with the value given by Leonard and Boring (*63*).

[b] Threshold energy for the formation of diatomic ions by associative ionization.

tion of those of methane. The curves show a slight shoulder at about 22 eV electron energy.

Figure 11 shows a small effect of chemical isomerism on the *W* values. The results for *n*-butane are clearly lower than those for i-butane between 13 and 80 eV in spite of the higher ionization threshold of *n*-butane. Meisels (*5*) reported that for 1-MeV electrons the *W* value is 0.1 eV lower in *n*-butane than in i-butane.

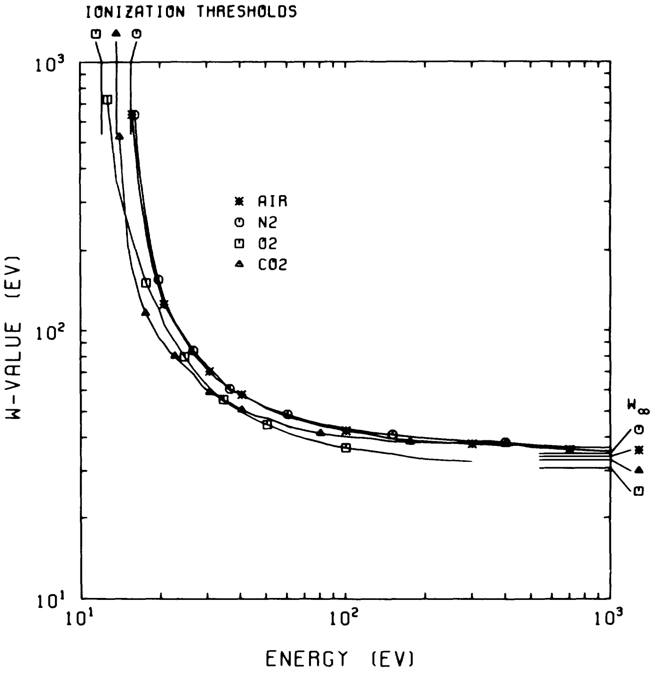

FIG. 7. Air and its components.

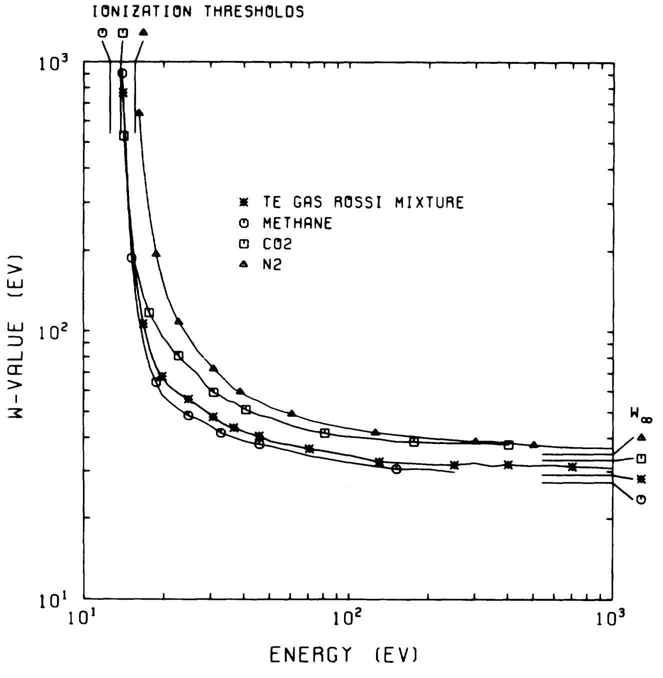

FIG. 8. Tissue equivalent gas (Rossi–Failla mixture) and its components.

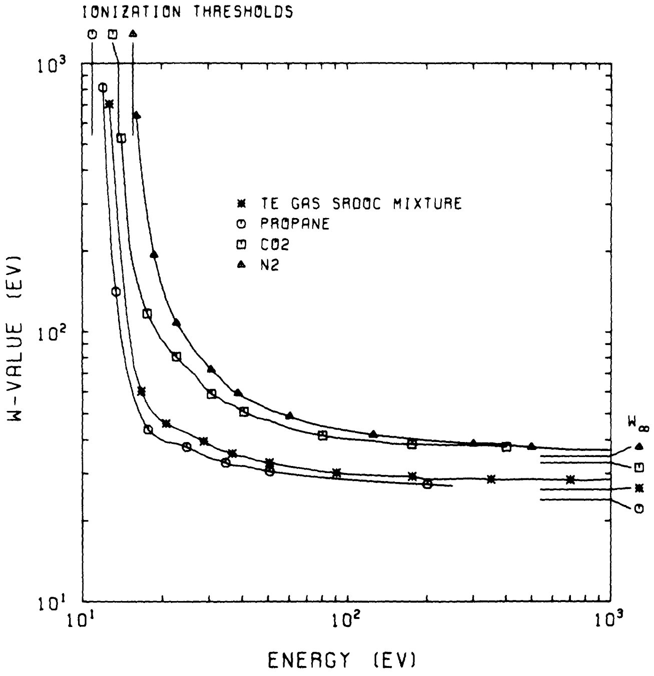

FIG. 9. Tissue equivalent gas (Srdoc mixture) and its components.

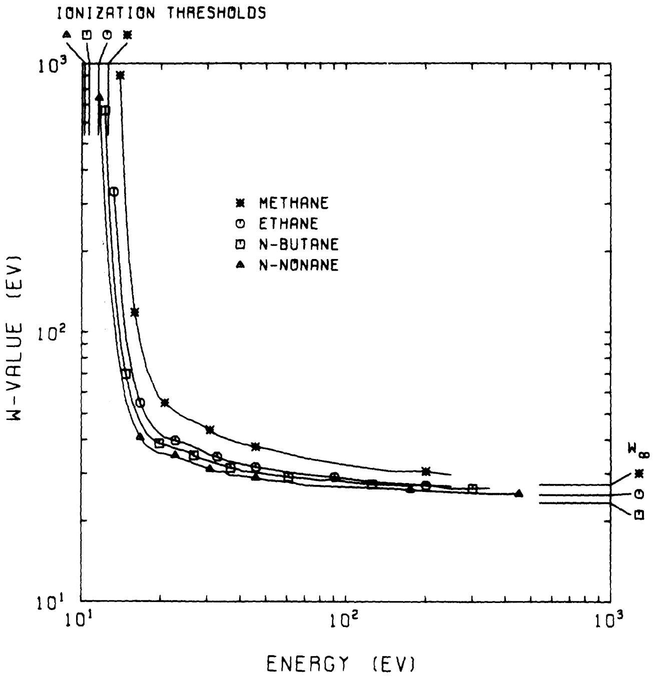

FIG. 10. Alkanes.

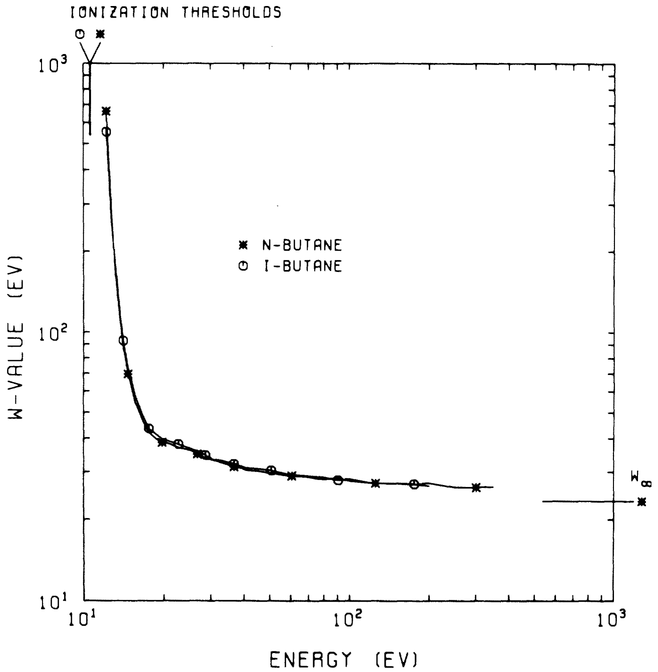

FIG. 11. Isomerism effect in butane.

Figure 12 shows the results for the compounds C_2H_6, C_2H_4, and C_2H_2. As the configuration of the outer-shell electrons is different in these molecules, different curve shapes are to be expected. The same holds for CH_3COCH_3 and C_2H_5OH, as shown in Fig. 13.

Figure 14 shows isotope effects in hydrogen, water vapor, and benzene. In water vapor and benzene the deuterated molecules have significantly lower *W* values, while the difference between hydrogen and deuterium is not marked. The isotope effect was predicted by Platzman (*6*) and experimentally proved by Jesse (*7*) for β particles from ^{63}Ni and by Meyerson (*8*) for 70-eV electrons. It is caused by "superexcited" states of a molecule which lie above the ionization threshold. These states decay by two competing processes, either by production of an ion pair through preionization or by an atomic rearrangement (for example, the dissociation of the molecule). For the undeuterated molecules the pathway to the dissociation is more probable than for the deuterated molecules because of their lower reduced mass. Therefore the superexcited deuterated molecules decay with higher probability into an ionized state than the undeuterated molecules and show lower *W* values. Jesse proposed, based on the energy dependence of the isotope effect in the ionization of hydrocarbons by α particles (*9*), that superexcited states would be produced preferentially by low-energy electrons. The results in Fig. 14 show that in fact the isotope effect is much more pronounced for low energies; only when very close to the ionization threshold does it decrease again as the superexcited levels lie above this threshold.

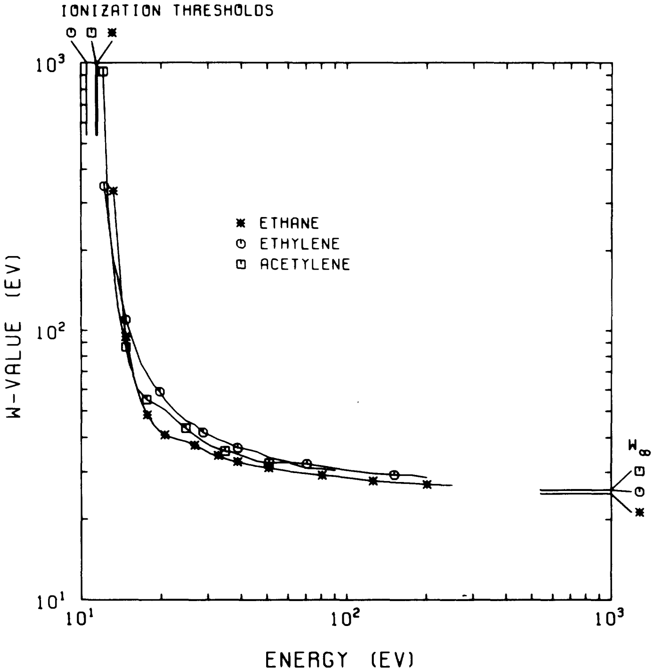

FIG. 12. Ethane, ethylene, and acetylene.

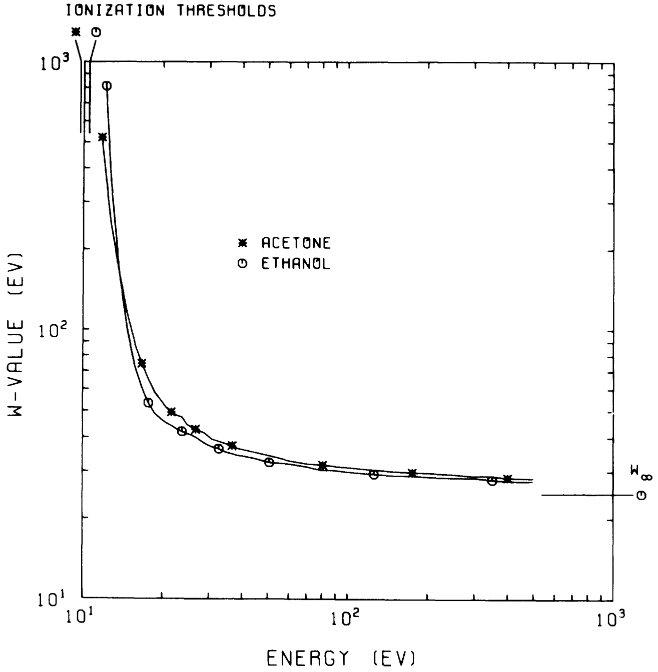

FIG. 13. Acetone and ethanol.

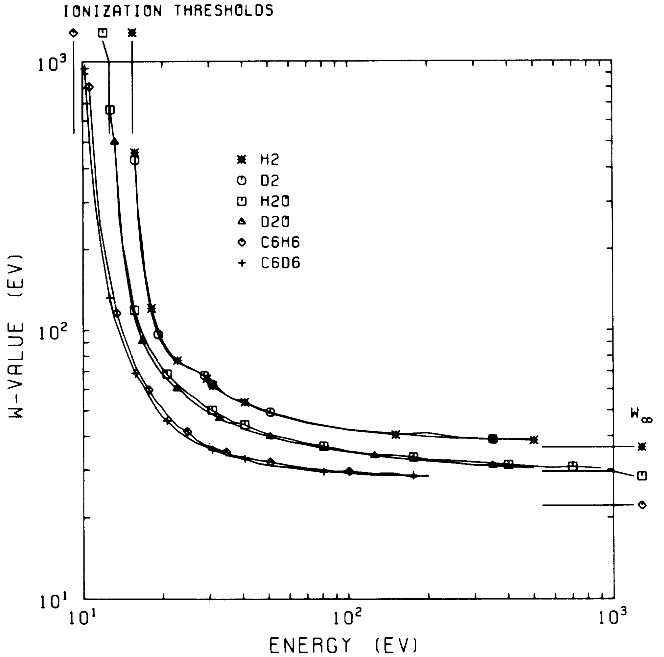

FIG. 14. Isotope effects in hydrogen, water vapor, and benzene.

Figure 15 shows the results for three rare gases. They are similar to each other with slight shoulders at electron energies a few electron volts below twice the ionization potential. The ionization is not zero at the ionization threshold. For rare gases the ion production limit at low energy is not determined by the atomic ionization thresholds indicated by full lines, but by the thresholds for the associative ionization indicated by broken lines. In this process diatomic rare gas ions are formed from excited atoms:

$$X^* + X \rightarrow X_2^+ + e^-.$$

It was investigated by Hornbeck and Molnar (*10*) in a mass spectrometer experiment at pressures as low as 10^{-4} mbar—much lower than the pressures used in this experiment. Investigations of the effect are summarized for all rare gases by Hurst and Klots (*11*). Extensive measurements for argon, krypton, and xenon have been carried out by Huffman and Katayama (*12*), who have measured precisely the threshold excitation energy for ion production using the photoexcitation method (see Table II). These authors have also measured the product of the effective radiative lifetime of the excited argon levels and the diatomic-ion-formation rate constant. They found values of 3.6×10^{-18} to 1.28×10^{-16} cm^3/atom for different levels. In the *W*-value measurements for argon below the ionization threshold the maximum of the current ratio (see Fig. 6) was found at a gas density of about 3×10^{15} atoms/cm^3. At this density an increase of the ionization current with increasing pressure would be expected. Surprisingly this was not found; the ratio showed the same slope as that shown in Fig. 6. Presumably the larger dimensions of the present apparatus increase the effective radiative lifetime of the argon

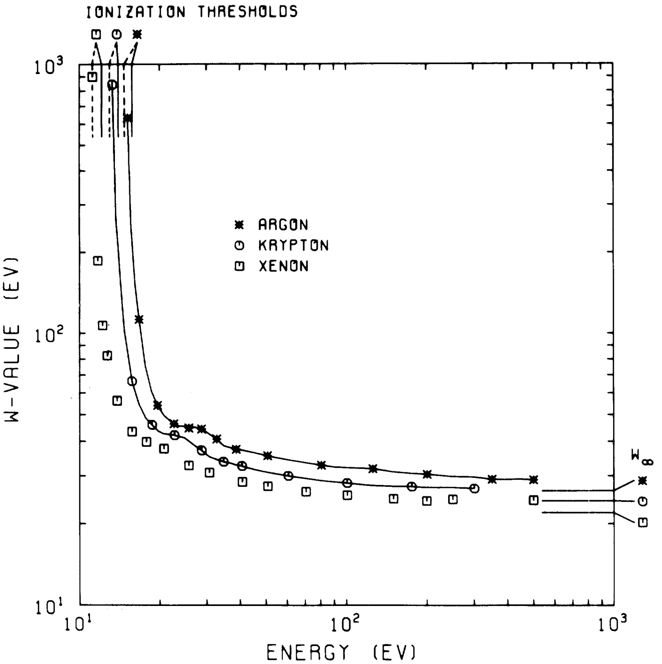

Fig. 15. Rare gases.

levels, so that the pressure dependence of the associative ionization is superimposed by the increasing part of the ratio, and in the linear part saturation has already occurred.

In the following, some results will be compared with experimental and theoretical data of other authors.

Figure 16 shows some data for air. An excellent agreement is found with the latest results by Waibel and Grosswendt (*13*). The older results by Cole (*14*), Gerbes (*15*), and Breunig (*16*) show relatively high deviations. A satisfying agreement with recent calculations by Paretzke and Berger (*17*) is also found in water vapor (Fig. 17).

For hydrogen the agreement with the old experimental work by Johnson (*18*) is surprisingly good (Fig. 18). The electron gun used by Johnson is similar to the one used in this work. The comparison with theoretical results gives good agreement with Spencer and Pal (*19*) above 30 eV, with Cravens *et al.* (*20*) above 80 eV, and with Garvey and Green (*21*) and Jones (*22*) above 150 eV. The peak predicted theoretically by Spencer and also by Cravens at about 25 eV cannot be found; however, there is a slight shoulder. The values calculated by Gerhart (*23*) are higher but show a similar slope. Two theoretical curves calculated by Douthat (*24*) which correspond to different assumptions about triplet excitation cross sections show partial agreement with the experiments. One curve has a similar slope and agrees well above 60 eV; the other agrees well down to 30 eV but has a different slope below this energy. The results for CH_4 join well with those by Srdoc and Obelic (*25*)

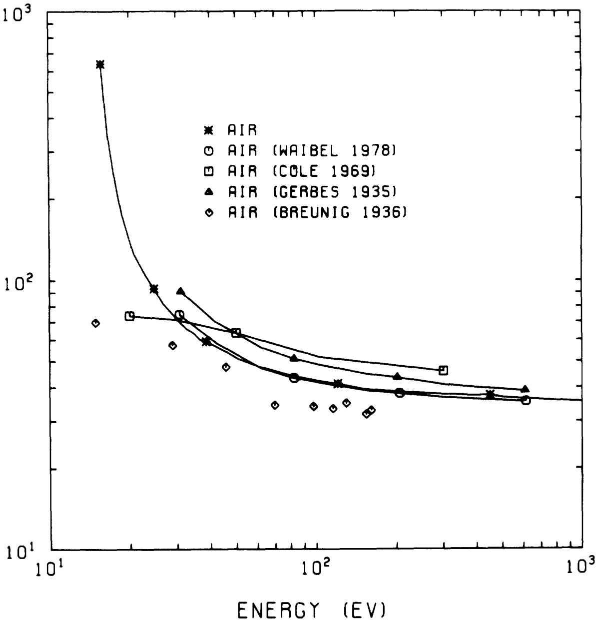

FIG. 16. Air.

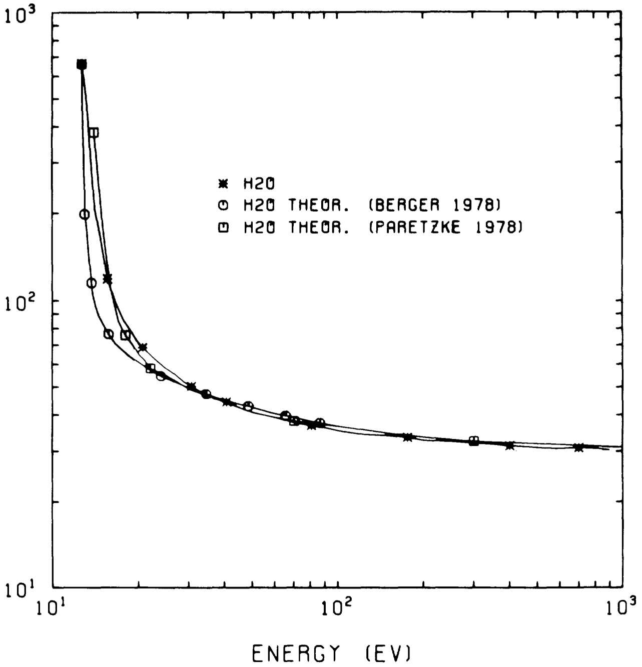

FIG. 17. Water vapor.

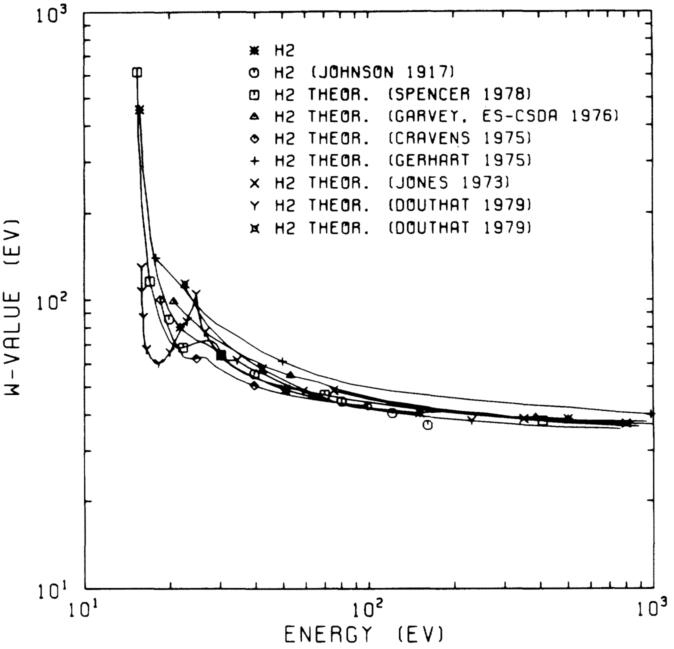

FIG. 18. Hydrogen.

above 250 eV (Fig. 19), although these are calculated from photon *W* values, whereas the agreement with experimental results by Smith and Booz (*26*) and with calculations by Dayashankar (*27*) is not good.

For N_2 (Fig. 20) good agreement was found only with the theoretical results obtained by Khare and Kumar (*28*), who integrated the Fowler equation. A comparison with the experimental results of Smith and Booz (*26*), Pigge (*29*), and Johnson (*18*) shows less agreement.

A comparison of the results for argon (Fig. 21) with several theoretical calculations shows a good agreement at about 30 eV and a slightly increasing difference at higher energies.The theoretical curves by Fox *et al.* (*30*) and Parikh[1] agree well with each other above 30 eV and with those of Eggarter (*31*) starting at 35 eV and Unnikrishnan and Prasad (*32*) starting at 30 eV electron energy. The latter two works are not shown in Fig. 21 for clearness. Below 30 eV the calculations by Fox and by Parikh show a minimum, where a shoulder is found experimentally, and convergence to the atomic ionization threshold, since associative ionization is not considered in the calculations.

A comparison of the results for xenon with the experimental work by Samson and Haddad (*33*) for CO_2 (Fig. 22) with that by Smith and Booz (*26*) and for TE gas (Fig. 23) with the same work, with that by Waker and Booz (*34*), and with the calculation by Dayashankar (*35*) shows occasional agreement. Inokuti predicted theo-

---

[1] M. Parikh, Energetic electron degradation spectra and initial yields in argon. IBM Research Report RJ2711 (34606), 1979.

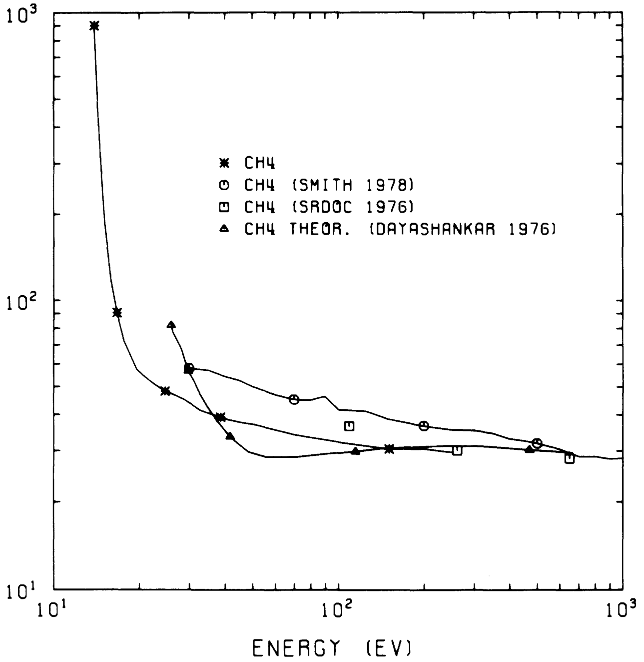

FIG. 19. Methane.

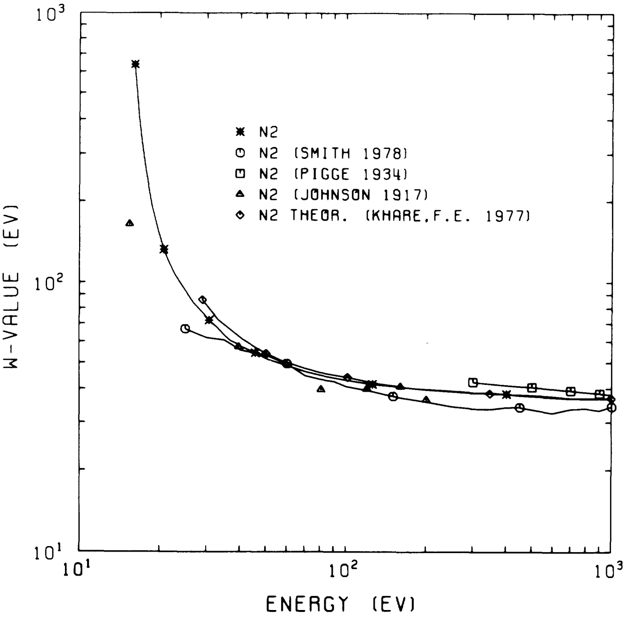

FIG. 20. Nitrogen.

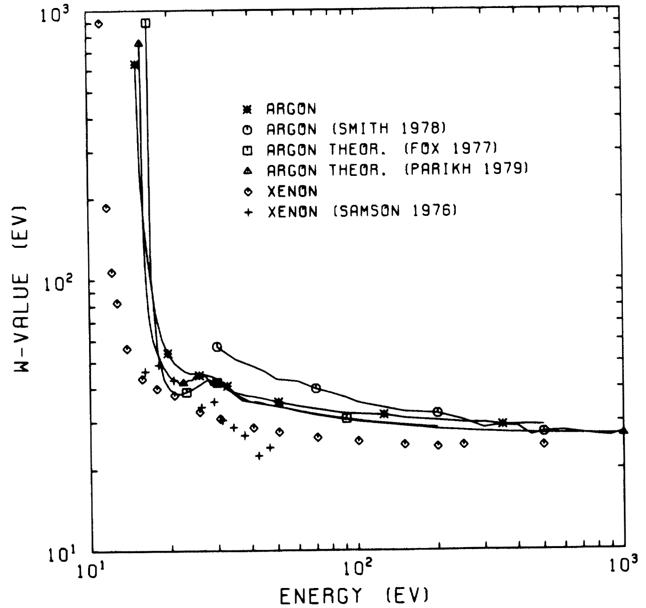

FIG. 21. Argon and xenon.

retically (*36*) that the number of ions produced by low-energy electrons should rise linearly with the electron energy at energies exceeding some multiples of the ionization threshold according to the formula,

$$N_i(E) = \frac{E}{W} = \frac{E - U}{W_a},$$

where W_a is the high-energy W value and U is the mean energy of the subionization electrons. Analysis of the measured data shows that in the energy region of the present experiments the value W_a is a little higher but very close to the high-energy W value for all gases. The deviation varies between 0 and +10%. As an example, the curves for H_2 and CH_4 are shown in Fig. 24. The W_a are 37.0 eV for H_2 and 28.5 eV for CH_4.

ERROR DISCUSSION

Three sources of errors can influence the accuracy of the W-value measurements:

(1) an error in the determination of the electron energy and the electron current;
(2) an error in the measurement of the ion current;
(3) impurities in the investigated gases.

The determination of the electron energy and the measurement of the current were tested under vacuum conditions, as described in an earlier section. The energy of the electrons is determined by the cathode voltage, the thermal spread, and the contact potential. In Fig. 4 it is shown that 80% of the electrons have an energy between 0.4 and 1.2 eV, and 1% of them have even more than 1.7 eV above the applied

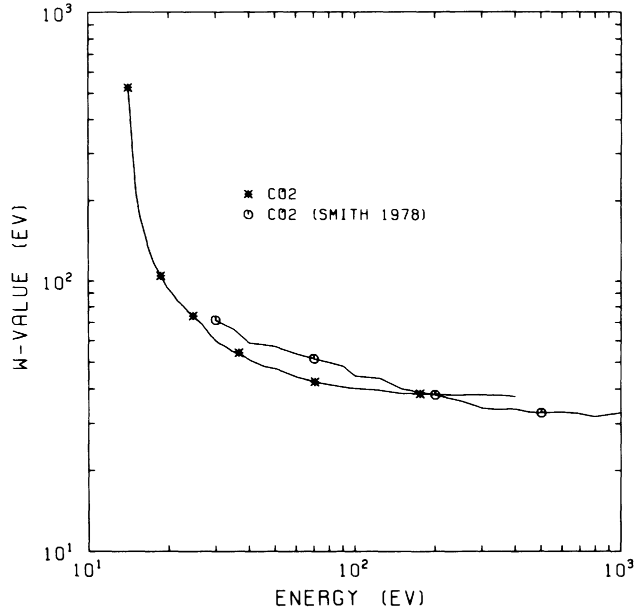

FIG. 22. Carbon dioxide.

voltage. The thermal spread of the spectrum may produce an error in the region where the *W* value depends strongly on the electron energy. The energy error produced by this spread was calculated for some gases; it is less than 0.3 eV. The cathode voltage is produced with a precise high voltage supply and measured with a digital voltage meter with 0.1% accuracy. The ratio of the ion current and the electron gun current is measured with an accuracy of better than 0.2%. The current measurement assemblies are regularly calibrated with a constant current from a pA-source and are operated in the same range to avoid calibration errors.

An important source of errors is the extrapolation to zero pressure. It is accurate only if the decrease of the pressure dependence curve (Fig. 6) is linear and not too steep. The steepness was no problem in any of the cases, but in some organic gases the linear part showed a slight curvature at higher energies. If the estimated uncertainty of the linear extrapolation was more than 1%, the results were rejected (for example, in acetylene the results above 80 eV). A principal objection to the linear extrapolation of the ratio to zero pressure is that its correctness cannot be proved experimentally. The decrease of the ratio is caused by scattering of electrons within the gun and by ion collection by the cathode. This decrease will be nonlinear if:

(a) The energy is too high. The occurrence of nonlinearity is an indicator for the high-energy limit of the usefulness of the unpumped gun.

(b) The collection of ions by the gun is influenced by space charges produced by these ions. In this case the ratio should be dependent not only on the pressure but also on the gun current. This has been excluded by test measurements.

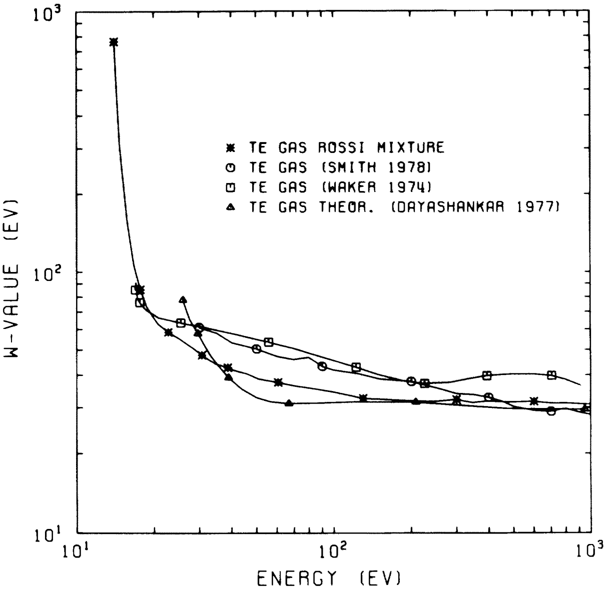

FIG. 23. Tissue-equivalent gas (Rossi–Failla mixture).

(c) Interactions between excited or ionized particles among one another influence the ratio. In this case the ratio should also depend on the gun current.

The influence of all these effects should increase with increasing pressure. This leads to the conclusion that in all cases where a clear linear part in the pressure dependence curve is seen, the extrapolation of this part to zero pressure yields the correct results.

A further source of errors is electron backscattering in the gas to the electron gun. With the data measured by Waibel and Grosswendt (*13*) the backscatter ratio was estimated at various gas pressures. Even with extrapolation to zero pressure an error of 0.1–0.2% remains because of a slight nonlinearity of the pressure dependence of electron backscattering to the gun.

The ion current measurement may be influenced by recombination and by gas amplification in the field of the ion collector wire. Normally recombination need not be considered at the low pressure used in the experiments, but during the pulsing time low-energy electrons may be captured in the ion cloud, so that the recombination probability is higher than in an unpulsed ion chamber. Tests with various collecting voltages between 20 and 100 V, gun currents between 0.2 and 1.2 nA, and pulsing times between 3 and 8 μsec yielded nonsystematic deviations of 0.7% from the mean value. Even in oxygen, which may produce negative ions, no higher deviation was found. Gas amplification starts at collecting voltages above 120 V; at 60 V it is negligible. A small error is produced by electron capture by the ion collector wire during the pulsing time. This lowers the ion current, as first, a negative charge reaches the wire, and second, energetic scattered electrons are stopped in the wire instead of in the gas. This error was calculated with a Monte

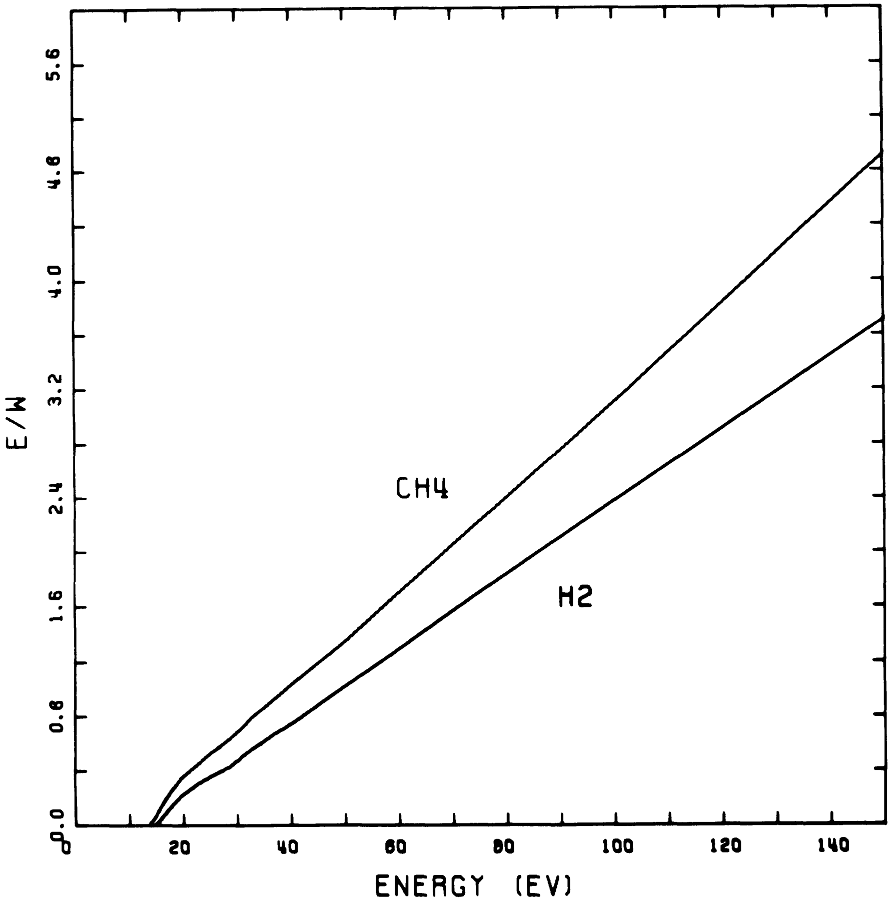

FIG. 24. The number of ions produced by electrons in methane and in hydrogen.

Carlo program by Paretzke and Leuthold[2] for various electron energies. By extrapolation to zero pressure the remaining error is less than 0.2%. Test measurements were carried out at energies below the ionization thresholds with 11.7-eV electrons in TE gas (Rossi mixture) and with 13.6-eV electrons in nitrogen. The ratio of the electron current in the ion collector wire to the gun current, extrapolated to zero pressure, was 0.0004 in both cases.

In most of the gases slight impurities may be neglected; their influence is given by the formula by Strickler (*37*). Only in the rare gases do they play an important role because of the so-called Jesse effect (*38*). The rare gases have high-lying metastable and resonant states which store excitation energy until they collide with an impurity molecule which may be ionized by energy transfer. This effect was investigated extensively by Payne *et al.* (*39*) for helium and neon and by Hurst *et al.*

---

[2] H. G. Paretzke and G. Leuthold, private communication.

(*40*) for argon. The impurities in the present measurements are so low that the Jesse effect in the three investigated rare gases should be negligible, since no ionization is found below the threshold for the associative ionization. This error analysis, the good agreement of some measurements with newer experiments and calculations carried out independently by other authors, and the asymptotic behavior of the *W*-value curves at high energies and near the thresholds lead to the conclusion that the total experimental error is less than 2% in the *W* values and less than 0.4 eV in the energy.

ACKNOWLEDGMENTS

The author wishes to thank Professor W. Jacobi for his inspiration and interest in this work; Drs. G. Burger, M. Inokuti, and H. Bichsel for many discussions and suggestions; Mr. G. Leuthold for some calculations; Mr. H. Mathes for the execution of many experiments; and Professor F. Lenz and his co-workers (University of Tuebingen) for providing computer programs for electron pathway calculations.

RECEIVED: September 28, 1979; REVISED: June 4, 1980; RE-REVISED: June 30, 1980

REFERENCES

1. F. KOHLRAUSCH, *Praktische Physik*, Vol. 3, p. 95. Teubner, Stuttgart, 1968.

2. D. COMBECHER, W-values of low energy electrons for several gases. In *Proceedings, Third Symposium on Neutron Dosimetry in Biology and Medicine, Neuherberg/München* (G. Burger and H. G. Ebert, Eds.), pp. 97–106. Commission of the European Communities, Luxembourg, 1978. [EUR 5848 d-e-f.]

3. R. W. KISER, *Tables of Ionization Potential.* Report TID-6142, USAEC Division of Technical Information Extension, Oak Ridge, TN, 1960. [Available from National Information Service, Springfield, VA 22161.]

4. H. M. ROSENSTOCK, K. DRAXL, B. W. STEINER, and J. T. HERRON, Energetics of gaseous ions. *J. Phys. Chem. Ref. Data* **6** (1977).

5. G. G. MEISELS, Gas phase dosimetry by use of ionization measurements. *J. Chem. Phys.* **41,** 51–56 (1964).

6. R. L. PLATZMAN, Superexcited states of molecules, and the primary action of ionizing radiation. *Vortex* **23,** 372–389 (1962).

7. W. P. JESSE, Isotope effect in the ionization of polyatomic gases by beta particles. *J. Chem. Phys.* **38,** 2774–2775 (1963).

8. S. MEYERSON, H. M. GRUBB, and R. W. VANDER HAAR, Effects of isotopic labeling and molecular structure on probability of ionization by electron impact. *J. Chem. Phys.* **39,** 1445–1446 (1963).

9. W. P. JESSE, Isotope effect as a function of alpha particle energy in the ionization of hydrocarbon gases. *J. Chem. Phys.* **52,** 1314–1316 (1970).

10. J. A. HORNBECK and J. P. MOLNAR, Mass spectrometric studies of molecular ions in the noble gases. *Phys. Rev.* **84,** 621–625 (1951).

11. G. S. HURST and C. E. KLOTS, Elementary processes in irradiated noble gases. In *Advances in Radiation Chemistry* (M. Burton and J. L. Magee, Eds.), Vol. 5, pp. 1–97. Wiley, New York, 1976.

12. R. E. HUFFMAN and D. H. KATAYAMA, Photoionization study of diatomic-ion formation in argon, krypton, and xenon. *J. Chem. Phys.* **45,** 138–146 (1966).

13. E. WAIBEL and B. GROSSWENDT, Determination of W values and backscatter coefficients for slow electrons in air. *Radiat. Res.* **76,** 241–249 (1978).

14. A. COLE, Absorption of 20-eV to 50,000-eV electron beams in air and plastic. *Radiat. Res.* **38,** 7–33 (1969).

15. W. Gerbes, Ueber die Ionisierungswirkung von Kathodenstrahlen in Luft. *Ann. Phys. (Leipzig)* **23,** 648–656 (1935).
16. E. Breunig, Die totale Traegerbildung langsamer Kathodenstrahlen in der Naehe der Traegerbildungsspannung. *Ann. Phys. (Leipzig)* **25,** 467–480 (1936).
17. H. G. Paretzke and M. J. Berger, Stopping power and energy degradation for electrons in water vapor. In *Proceedings, Sixth Symposium on Microdosimetry, Brussels* (J. Booz and H. G. Ebert, Eds.), pp. 749–758. Commission of the European Communities, Harwood, London, 1978. [EUR 6064 d-e-f.]
18. J. B. Johnson, Total ionization by slow electrons. *Phys. Rev. II* **10,** 609–623 (1917).
19. L. V. Spencer and R. Pal, *Numeric Solution of the Electron Slowing-Down Equation for Molecular Hydrogen.* Report NBSIR 78-1523, National Bureau of Standards, Washington, DC, 1978.
20. T. E. Cravens, G. A. Victor, and A. Dalgarno, The absorption of energetic electrons by molecular hydrogen gas. *Planet. Space Sci.* **23,** 1059–1070 (1975).
21. R. H. Garvey and A. E. S. Green, Energy apportionment techniques based upon detailed atomic cross sections. *Phys. Rev. A* **14,** 946–953 (1976).
22. W. M. Jones, Some calculated quantities in the radiation chemistry of molecular hydrogen: Average energy per ion pair and numbers of singlet and triplet excitations per ion pair. *J. Chem. Phys.* **59,** 5688–5695 (1973).
23. D. E. Gerhart, Comprehensive optical and collision data for radiation action. I. H_2. *J. Chem. Phys.* **62,** 821–832 (1975).
24. D. A. Douthat, Energy deposition and electron energy degradation in molecular hydrogen. *J. Phys. B* **12,** 663–678 (1979).
25. D. Srdoc and B. Obelic, Measurement of W at very low photon energy. In *Proceedings, Fifth Symposium on Microdosimetry, Verbania-Pallanza* (J. Booz, H. G. Ebert, and B. G. R. Smith, Eds.), pp. 1007–1021. Commission of the European Communities, Luxembourg, 1976. [EUR 5452 d-e-f.]
26. B. G. R. Smith and J. Booz, Experimental results on W-values and transmission of low energy electrons in gases. In *Proceedings, Sixth Symposium on Microdosimetry, Brussels* (J. Booz and H. G. Ebert, Eds.), pp. 759–775. Commission of the European Communities, Harwood, London, 1978. [EUR 6064 d-e-f.]
27. Dayashankar, Mean energy expended per ion pair formed in methane by electrons. *J. Mysore Univ. Sect. B* **26,** 181–185 (1977).
28. S. P. Khare and A. Kumar, Jr., Mean energy expended per ion pair by electrons in molecular nitrogen. *J. Phys. B* **10,** 2239–2251 (1977).
29. H. Pigge, Ionisierungswirkung langsamer Kathodenstrahlen. *Ann. Phys. (Leipzig)* **20,** 233–249 (1934).
30. J. L. Fox, A. Dalgarno, and G. A. Victor, The absorption of energetic electrons by argon gas. *Planet. Space Sci.* **25,** 71–78 (1977).
31. E. Eggarter, Comprehensive optical and collision data for radiation action. II. Ar. *J. Chem. Phys.* **62,** 833–847 (1975).
32. K. Unnikrishnan and M. A. Prasad, Energy deposition by electrons in argon. *Radiat. Res.* **80,** 225–232 (1979).
33. J. A. R. Samson and G. N. Haddad, Average energy loss per ion pair formation by photon and electron impact on xenon between threshold and 90 eV. *Radiat. Res.* **66,** 1–10 (1976).
34. A. J. Waker and J. Booz, Measurement of the W-value of low energy electrons. In *Proceedings, Second Symposium on Neutron Dosimetry in Biology and Medicine, Neuherberg/München* (G. Burger and H. G. Ebert, Eds.), pp. 455–478. Commission of the European Communities, Luxembourg, 1974. [EUR 5273 d-e-f.]
35. Dayashankar, Calculation of W for low energy electrons in tissue-equivalent gas. *Health Phys.* **33,** 465–470 (1977).
36. M. Inokuti, Ionization yields in gases under electron irradiation. *Radiat. Res.* **64,** 6–22 (1975).
37. T. D. Strickler, Ionization by alpha particles in binary gas mixtures. *J. Phys. Chem.* **67,** 825–830 (1963).

38. W. P. Jesse and J. Sadauskis, Alpha-particle ionization in mixtures of noble gases. *Phys. Rev.* **88**, 417–418 (1952).

39. M. G. Payne, G. S. Hurst, M. H. Nayfeh, J. P. Judish, C. H. Chen, E. B. Wagner, and J. P. Young, Kinetics of He(2^1S) using resonance ionization spectroscopy. *Phys. Rev. Lett.* **35**, 1154–1156 (1975).

40. G. S. Hurst, T. E. Bortner, and R. E. Glick, Ionization and excitation of argon with alpha particles. *J. Chem. Phys.* **42**, 713–719 (1965).

41. R. E. Worley and F. A. Jenkins, A new Rydberg series in N_2. *Phys. Rev.* **54**, 305 (1938).

42. K. Watanabe, Ionization potentials of some molecules. *J. Chem. Phys.* **26**, 542–547 (1957).

43. R. S. Nakata, K. Watanabe, and F. M. Matsunaga, Absorption and photoionization coefficients of CO_2 in the region 580–1670 Å. *Sci. Light (Tokyo)* **14**, 54 (1965).

44. B. Brehm, Massenspektrometrische Untersuchungen der Photoionisation von Molekuelen. *Z. Naturforsch. Teil A* **21**, 196 (1966).

45. A. J. C. Nicholson, Photoionization-efficiency curves. II. False and genuine structure. *J. Chem. Phys.* **43**, 1171–1177 (1965).

46. W. A. Chupka and J. Berkowitz, Photoionization of ethane, propane, and n-butane with mass analysis. *J. Chem. Phys.* **47**, 2921–2933 (1967).

47. K. Watanabe, T. Nakayama, and J. Mottl, Ionization potentials of some molecules. *J. Quant. Spectrosc. Radiat. Transfer* **2**, 369 (1962).

48. R. E. Honig, Ionization potentials of some hydrocarbon series. *J. Chem. Phys.* **16**, 105–112 (1948).

49. A. D. Walsh, The absorption spectrum of acetaldehyde in the vacuum ultra-violet. *Proc. Roy. Soc. London Ser. A* **185**, 176 (1946).

50. G. L. Weissler, Photoionization in gases and photoelectric emission from solids. *Handb. Physik* **21**, 304–382 (1956).

51. V. H. Dibeler, R. M. Reese, and M. Krauss, Mass-spectrometric study of photoionization. II. H_2, HD, and D_2. *J. Chem. Phys.* **42**, 2045–2048 (1965).

52. P. G. Wilkinson, Absorption spectra and ionization potentials of benzene and benzene-d_6. *J. Chem. Phys.* **24**, 917 (1956).

53. C. E. Moore, *Ionization Potentials and Ionization Limits Derived from the Analysis of Optical Spectra.* Report NSRDS-NBS 34, National Bureau of Standards, Washington, DC, 1970.

54. W. P. Jesse, Absolute energy to produce an ion pair in various gases by beta-particles from ^{35}S. *Phys. Rev.* **109**, 2002–2004 (1958).

55. R. L. Platzman, Total ionization in gases by high-energy particles: An appraisal of our understanding. *Int. J. Appl. Radiat. Isot.* **10**, 116–127 (1961).

56. J. Weiss and W. Bernstein, The current status of W, the energy to produce one ion pair in a gas. *Radiat. Res.* **6**, 603–610 (1957).

57. P. Adler and H. K. Bothe, Der Ionisierungsaufwand W organischer Molekuele und seine Abhaengigkeit von der Molekuelstruktur. *Z. Naturforsch. Teil A* **20**, 1700–1707 (1965).

58. M. Leblanc and J. A. Herman, Determination des valeurs W_{beta} pour les gaz et vapeurs organiques par la methode des courants de saturation. *J. Chim. Phys.* **21**, 1055–1060 (1966).

59. R. Cooper and R. M. Mooring, Ionization current measurements and the energy required to form an ion pair in gamma-ray irradiated gases. *Aust. J. Chem.* **21**, 2417–2425 (1968).

60. K. P. Schulze, Messung der effektiven Ionisierungsenergie in Gasen. *Atomkernenergie* **11**, 397–403 (1966).

61. T. A. Stoneham, D. R. Ethridge, and G. G. Meisels, Precise measurement of W, the mean energy required for ion pair formation in gases. I. Alkanes. *J. Chem. Phys.* **54**, 4054–4059 (1971).

62. G. G. Meisels and D. R. Ethridge, Precise measurements of W, the average energy required for ion pair formation. II. Alcohols and water. *J. Phys. Chem.* **76**, 3842–3846 (1972).

63. B. E. Leonard and J. W. Boring, The average energy per ion pair, W, for hydrogen and oxygen ions in a tissue equivalent gas. *Radiat. Res.* **55**, 1–9 (1973).